Turbulent Diffusion of Heat and Mass in Catalytic Reactors for Hydrazine Decomposition

ARTHUR S. KESTEN*
United Aircraft Research Laboratories, East Hartford, Conn.

An analytical study of catalyzed hydrazine decomposition reaction chambers was performed to assess the effects on the steady-state behavior of the system of nonuniform radial injection and of catalyst bed configurations exhibiting both radial and axial nonuniformities. Radial variations in mass flow rate or bed packing cause radial temperature and concentration gradients that lead to turbulent diffusion of heat and mass in the reactor system. A computer program was developed to calculate temperature and reactant concentration distributions as functions of axial and radial position in typical hydrazine reaction chambers. The program is based upon a model of the reactor system that includes treatment of the turbulent diffusion of heat and mass in the free-gas phase along with heat and mass diffusion within the catalyst particles and between the particles and the free-gas phase. Both thermal and catalytic decomposition of the reactants are considered. It was shown that a one-dimensional model of the system based on parameters averaged over the reactor cross section, is not adequate to describe the behavior of a reactor which exhibits significant radial variations in injection profile or bed configuration. For these systems, it is necessary to use the two-dimensional model to effectively predict, for example, reactor locations where hydrazine diffusion from low- to high-temperature regions results in unusually high temperatures at the interface between the regions.

Nomenclature

a = radius of spherical particle, ft
A_p = total external surface of catalyst particle per unit volume of bed, ft^{-1}
c = reactant concentration lb/ft^3
C_f = specific heat of fluid in the interstitial phase; $\overline{C_f}$ = average value, Btu/lb-°R
D = diffusion coefficient of reactant gas, ft^2/sec
F = rate of feed of hydrazine from distributed injectors into the system, lb/ft^3-sec
g_c = conversion factor $(lbm/lbf)\ ft/sec^2$
G = mass flow rate, lb/ft^2-sec
h = enthalpy, Btu/lb
$\mathcal{H}_c$ = heat-transfer coefficient, Btu/ft^2-sec-°R
H = heat of reaction (negative for exothermic reaction), Btu/lb
k_c = mass transfer coefficient, fps
K_p = thermal conductivity of the porous catalyst particle, Btu/ft-sec-°R
M = molecular weight; $\bar{M}$ = average molecular weight
N_r = radial mass flux, lb/ft^2-sec
P = chamber pressure, psia
q_r = radial heat flux, Btu/ft^2-sec
r = radial distance, ft
r_{het} = rate of (heterogeneous) chemical reaction on the catalyst surfaces, lb/ft^3-sec
r_{hom} = rate of (homogeneous) chemical reaction in the interstitial phase, lb/ft^3-sec
R = radius of reactor, ft
T = temperature, °R
w_i = weight fraction of reactant in interstitial phase
X_A, X_H = mole fractions of ammonia and hydrazine, respectively, in interstitial phase
x = radial distance from the center of the spherical catalyst particle, ft
z = axial distance, ft
δ = interparticle void fraction
ϵ = eddy diffusivity, ft^2/sec
λ = eddy conductivity, Btu/ft-sec-°R
μ = viscosity of interstitial fluid, lb/ft-sec
ρ_i = density of interstitial fluid, lb/ft^3

Subscripts

F = feed
i = interstitial phase
p = gas within the porous catalyst particle
s = surface of catalyst particle

Superscripts

J = chemical species
L = liquid at vaporization temperature
V = vapor at vaporization temperature

Introduction

ANALYTICAL studies that characterize the behavior of catalytic reactors for hydrazine decomposition permit effective design of catalyzed monopropellant hydrazine rocket engines and gas generators. Studies previously reported in Refs. 1 and 2 included the development of computer programs that describe the steady-state and transient behavior of a reactor system in which complete radial mixing in the free-gas (or liquid) phase was assumed. These programs had been used to calculate temperature and reactant concentration distributions as functions of initial bed temperature, feed temperature, chamber pressure, mass flow rate, catalyst size distribution, and axial injector locations in a reactor packed with Shell 405 catalyst. In the present work, attention has been focused on extending the steady-state model to include radial as well as axial variations in temperature and concentrations in order to permit an analysis of various injection schemes and catalyst bed configurations that exhibit radial nonuniformities.

The analysis of a hydrazine engine reaction system pertains to a reaction chamber of arbitrary cross section packed with catalyst particles into which liquid hydrazine is injected at

Presented as Paper 69-421 at the AIAA 5th Propulsion Joint Specialist Conference, U.S. Air Force Academy, Colo., June 9–13, 1969; submitted May 26, 1969; revision received October 6, 1969. This work was performed by United Aircraft Research Laboratories for NASA under Contract NAS 7-458 initiated April 15, 1966.

* Supervisor, Kinetics and Heat Transfer Group.

arbitrarily selected locations. Catalyst particles are represented as "equivalent" spheres with a diameter taken as a function of the particle size and shape. Both thermal and catalytic vapor phase decompositions of hydrazine and ammonia are considered in developing equations describing the concentration distributions of these reactants. Diffusion of reactants from the free-gas phase to the outside surface of the catalyst pellets is taken into account. Since the catalyst material is impregnated on the interior and exterior surfaces of porous particles, the diffusion of reactants into the porous structure must also be considered. In addition, the conduction of heat within the porous particles must be taken into account since the decomposition reactions are accompanied by the evolution or absorption of heat.

Included in succeeding sections of this paper are detailed descriptions of 1) the development of a computer program representing a two-dimensional steady-state model of the reactor system and 2) the use of the two-dimensional program to calculate the effects on steady-state temperature and reactant concentration distributions of nonuniform radial injection and of catalyst bed configurations exhibiting both radial and axial nonuniformities.

Discussion

In developing the two-dimensional model of a hydrazine reactor system, the temperature and reactant concentrations in the bulk fluid phase are permitted to vary with radial and axial position in the reaction chamber. In the entrance region of the reactor, where the temperature is low enough to permit the existence of liquid hydrazine, radial mixing between adjacent layers of liquid is neglected. The equations representing the change in liquid enthalpy and temperature with axial distance at any radial position are the same as those developed for the one-dimensional model described in Ref. 1. As in the one-dimensional model, catalytic reaction is assumed to be fast enough to keep liquid hydrazine from wetting the pores of the particles; the hydrazine concentration at the surface of the catalyst particles at any location in the entrance region is then computed from the vapor pressure of liquid hydrazine in the interstitial phase at the same location.

In the vapor regions of the reaction chamber, turbulent diffusion of heat and mass is considered as a mechanism for radial mixing. Radial heat and mass fluxes are computed as functions of temperature and reactant concentration gradients. Heat is being supplied to the system by homogeneous as well as heterogeneous decomposition of hydrazine, and is being removed from the system by the catalytic decomposition of ammonia. The change in enthalpy with axial distance at any radial location is related to the reactant concentrations in the interstitial phase and at the surface of the porous catalyst particles by

$$\frac{\partial h_i}{\partial z} = -\frac{1}{G}\left\{F(h_i - h_F) + Ap\mathcal{H}_c[T_i - (T_p)_s] + H^{N_2H_4} r_{hom}^{N_2H_4}\delta + \frac{\partial q_r}{\partial r}\delta + \frac{q_r}{r}\delta + \frac{\partial T_i}{\partial r}\delta \sum_J N_r^J C_f^J\right\} \quad (1)\dagger$$

The changes in reactant weight fractions in the interstitial phase with axial distance at any radial location are related to the reactant concentrations in the interstitial phase and at the surface of the porous catalyst particles by

$$\frac{\partial w_i^{N_2H_4}}{\partial z} = \frac{1}{G}\left\{F - r_{hom}^{N_2H_4}\delta - A_p(k_c c_i)^{N_2H_4} - \frac{\partial N_r^{N_2H_4}}{\partial r}\delta - \frac{N_r^{N_2H_4}}{r}\delta - F\left(\frac{c_i}{\rho_i}\right)^{N_2H_4}\right\} \quad (2)$$

$$\frac{\partial w_i^{NH_3}}{\partial z} = \frac{1}{G}\left\{r_{hom}^{N_2H_4}\delta\frac{M^{NH_3}}{M^{N_2H_4}} + A_p(k_c c_i)^{N_2H_4}\times \frac{M^{NH_3}}{M^{N_2H_4}} - A_p\{k_c[c_i - (c_p)_s]\}^{NH_3} - \frac{\partial N_r^{NH_3}}{\partial r}\delta - \frac{N_r^{NH_3}}{r}\delta - F\left(\frac{c_i}{\rho_i}\right)^{NH_3}\right\} \quad (3)$$

$$\frac{\partial w_i^{N_2}}{\partial z} = \frac{1}{G}\left\{\frac{1}{2}r_{hom}^{N_2H_4}\delta\frac{M^{N_2}}{M^{N_2H_4}} + \frac{A_p}{2}\times (k_c c_i)^{N_2H_4}\frac{M^{N_2}}{M^{N_2H_4}} + \frac{A_p}{2}\{k_c[c_i - (c_p)_s]\}^{NH_3}\times \frac{M^{N_2}}{M^{NH_3}} - \frac{\partial N_r^{N_2}}{\partial r}\delta - \frac{N_r^{N_2}}{r}\delta - F\left(\frac{c_i}{\rho_i}\right)^{N_2}\right\} \quad (4)$$

$$\frac{\partial w_i^{H_2}}{\partial z} = \frac{1}{G}\left\{\frac{1}{2}r_{hom}^{N_2H_4}\delta\frac{M^{H_2}}{M^{N_2H_4}} + \frac{A_P}{2}\times (k_c c_i)^{N_2H_4}\frac{M^{H_2}}{M^{N_2H_4}} + \frac{3A_P}{2}\{k_c[c_i - (c_P)_S]\}^{NH_3}\times \frac{M^{H_2}}{M^{NH_3}} - \frac{\partial N_r^{H_2}}{\partial r}\delta - \frac{N_r^{H_2}}{r}\delta - F\left(\frac{c_i}{\rho_i}\right)^{H_2}\right\} \quad (5)$$

where

$$q_r = -\lambda(\partial T_i/\partial r) \quad (6)$$

$$N_r^J = -\epsilon(\partial c_i^J/\partial r)_r \quad (7)$$

$$\mathcal{H}_c = 0.74(G/A_p\mu)^{-0.41}(\overline{C_f}G/\rho_i) \quad (8)$$

$$k_c^J = (0.61G/\rho_i)(\mu/\rho_i D_i)^{-0.667}(G/A_p\mu)^{-0.41} \quad (9)$$

The eddy conductivity and diffusivity may be estimated from[4]

$$\lambda = a\overline{C_f}G/5\delta \quad \text{and} \quad \epsilon = aG/5\rho_i \quad (10)$$

The changes in reactant concentrations with axial distance are then given by

$$\partial c_i^J/\partial z = \rho_i\partial w_i^J/\partial z + (c_i^J/\rho_i)\partial\rho_i/\partial z \quad (11)$$

where

$$\partial\rho_i/\partial z = \rho_i[(1/\overline{M})\,\partial\overline{M}/\partial z - (1/T_i)\partial T_i/\partial z + (1/P)dP/dz] \quad (12)$$

$$\frac{1}{\overline{M}}\frac{\partial\overline{M}}{\partial z} = -\frac{1}{\sum_J (w_i^J/M^J)}\sum_J\frac{1}{M^J}\frac{\partial w_i^J}{\partial z} \quad (13)$$

and the pressure drop may be estimated from the Ergun equation[4] as

$$\frac{dP}{dz} = -\left(\frac{1-\delta}{\delta^3}\right)\left(1.75 + \frac{150(1-\delta)}{2aG/\mu}\right)\left(\frac{G^2}{2a\rho_i g_c}\right) \quad (14)$$

The mass flow rate G is computed as a function of the rate of feed of liquid hydrazine from the distributed injectors into the system. Radial pressure gradients, caused by particle-fluid viscous interaction, are neglected. Such pressure gradients would lead to recirculating flow patterns in the reaction chamber. This bulk radial flow is neglected in this analysis. It is assumed, therefore, that downstream of the injectors the mass flow rate profile remains unchanged.

Catalytic reaction of hydrazine on Shell 405 catalyst particles is so fast[1] that, even at low temperatures, the rate of decomposition of hydrazine vapor is controlled by the rate of diffusion of hydrazine from the bulk vapor through a stagnant gas film surrounding the catalyst particles to the outside surface of the particles. In the case of ammonia, however, film diffusion is fairly rapid relative to the rate of dissociation of ammonia within the particles. The concentration of ammonia at the surface of the catalyst particles, $(c_p)_s^{NH_3}$, is

† Equations of this type are presented in somewhat different form in Ref. 3. The last term on the right-hand side of the equation reflects the heat transferred by the radial diffusion of mass.

therefore significantly different from zero. The surface concentration can be calculated, along with the concentration profile in the porous particles, at any axial location in the reaction chamber by solving simultaneously the equation representing film and pore diffusion of heat and mass. In describing the diffusion of mass within a porous pellet, it is assumed that changes in the mass density of fluid within the particle are negligible relative to changes in concentration of the reacting species. In addition, pressure changes within the particle resulting from nonequimolar diffusion are neglected, as is heat transported by pore diffusion of mass. Assuming constant diffusion coefficients D_p and thermal conductivities K_p, the equations describing heat and mass transfer within a catalyst particle may be written as

$$D_p{}^{NH_3}\nabla^2 c_p{}^{NH_3} - r_{het}{}^{NH_3} = 0 \quad (15)$$

$$K_p\nabla^2 T_p - H^{NH_3} r_{het}{}^{NH_3} = 0 \quad (16)$$

The boundary conditions that consider diffusion of heat and mass through a film surrounding a spherical particle are

$$D_p{}^{NH_3}(dc_p/dx)_s{}^{NH_3} = k_c{}^{NH_3}[c_i{}^{NH_3} - (c_p)_s{}^{NH_3}] \quad (17)$$

and

$$(Hk_cc_i)^{N_2H_4} + H^{NH_3}D_p{}^{NH_3}(dc_p/dx)_s{}^{NH_3} = \mathfrak{H}_c[T_i - (T_p)_s] \quad (18)$$

where $(k_cc_i)^{N_2H_4}$ represents the rate of diffusion of hydrazine to the particle surface. It should be noted here that $(c_p)_s{}^{N_2H_4}$ is approximately zero, reflecting the fact that the catalytic decomposition of hydrazine vapor is quite rapid.

The temperature and ammonia concentration within a catalyst particle are related by[5]

$$T_p - (T_p)_s = -(H^{NH_3}D_p{}^{NH_3}/K_p)[(c_p)_s - c_p{}^{NH_3}] \quad (19)$$

The use of this relationship enables the reaction rate, $r_{het}{}^{NH_3}$, to be written as a function of concentration alone instead of concentration and temperature. In this case, however, the reaction rate is a function of two parameters $(T_p)_s$ and $(c_p)_s{}^{NH_3}$, which are yet to be determined. Equation (15) can be solved for the concentration at any point in the porous particle in terms of the reaction rate $r_{het}{}^{NH_3}$ and the interstitial concentration $c_i{}^{NH_3}$. The solution is derived in Refs. 2 and 6 as an implicit integral equation given by

$$c_p(x)^{NH_3} = c_i{}^{NH_3} - \left[\frac{1}{x} - \frac{ak_c{}^{NH_3} - D_p{}^{NH_3}}{a^2k_c{}^{NH_3}}\right] \times \int_0^x \xi^2 \frac{r_{het}{}^{NH_3}(c_p)}{D_p{}^{NH_3}}\,d\xi - \int_x^a \left[\frac{1}{\xi} - \frac{ak_c{}^{NH_3} - D_p{}^{NH_3}}{a^2k_c{}^{NH_3}}\right] \times \xi^2 \frac{r_{het}{}^{NH_3}(c_p)}{D_p{}^{NH_3}}\,d\xi \quad (20)$$

In order to determine the particle ammonia concentration profile directly in terms of the interstitial temperature and reactant concentrations it is necessary to solve Eqs. (17, 18, and 20) simultaneously. Numerical methods to accomplish this have been developed and programed for machine computation. These methods are described in detail in Ref. 7.

In the special case of negligible film resistance to heat and mass transfer [i.e., $(T_p)_s = T_i$ and $(c_p)_s = (c_i)$], Eq. (20) can be written, for any reacting species, as

$$c_p(x) = c_i - \left[\frac{1}{x} - \frac{1}{a}\right]\int_0^x \xi^2 \frac{r_{het}(c_p)}{D_p}\,d\xi - \int_x^a \left[\frac{1}{\xi} - \frac{1}{a}\right]\xi^2 \frac{r_{het}(c_p)}{D_p}\,d\xi \quad (21)$$

It is Eq. (21) that is used to describe the hydrazine concentration profiles within the catalyst particles located in the liquid region of the reaction chamber. In this liquid region it is assumed that liquid hydrazine wets the *outside* surface of the catalyst particles so that $(c_p)_s{}^{N_2H_4} = c_i{}^{N_2H_4}$, where $c_i{}^{N_2H_4}$ is the vapor concentration in equilibrium with liquid hydrazine at temperature T_i.

The equations representing the two-dimensional model have been programed for digital computation and a computer manual containing a detailed description of the operating characteristics of the program has been prepared.

Results and Calculations

A series of calculations was made using the two-dimensional steady-state computer program in order to examine the effectiveness of the two-dimensional model and to evaluate the effects on system performance of nonuniform radial injection and of catalyst bed configurations exhibiting both radial and axial nonuniformities. The calculated results in Figs. 1–4 refer to a 3-in.-diam reactor into which liquid hydrazine is injected at 530°R. Numerical values used for chemical rate constants, diffusivities and other parameters can be found in Ref. 7. Unfortunately, experimental data for comparison with the predicted temperature and concentration profiles is not available for systems exhibiting radial and axial nonuniformities.

Axial temperature profiles at various radial locations are plotted in Fig. 1a for a case in which a radial nonuniformity in mass flow rate G is represented as a step function. In this case, the upstream chamber pressure was taken as 100 psia and the catalyst bed packing was taken to consist of 25–30 mesh catalyst particles for the first 0.2 in. and $\frac{1}{8} \times \frac{1}{8}$-in. cylindrical pellets for the remainder of the bed. This configuration is referred to in the figures as the "standard bed configuration." Turbulent diffusion of heat, which tends to reduce radial temperature gradients, is more pronounced in the downstream end of the reactor. Here the catalyst particle size is larger, and both eddy conductivity and eddy diffusivity are directly proportional to particle size. The consequences of radial heat conduction are complicated somewhat by the simultaneous turbulent diffusion of mass. Higher temperatures are associated with more hydrazine decomposition; thus high-temperature regions may lose heat by radial conduction, but may gain hydrazine from adjoining low-temperature regions by radial diffusion of mass. Subsequent decomposition of this hydrazine may lead to even higher temperatures. In these same regions, the ammonia produced by the decomposition of hydrazine may exist at higher concentrations than in adjacent low-temperature regions. In the absence of radial diffusion the ammonia in these high-temperature regions would decompose and lower the temperature. With radial diffusion, however, the concentration of ammonia available for decomposition may be lowered considerably. For the case considered here, these combined effects lead to the temperature distribution shown in Fig. 1a.‡ For comparison purposes, the axial temperature profile corresponding to a radially uniform mass flow rate of 3.0 lb/ft²-sec is also plotted in Fig. 1a. This is the average mass flow rate calculated by averaging the actual mass flow rate profile over the cross-sectional area of the reactor. The mole-fraction distributions of hydrazine and ammonia associated with the temperature distribution shown in Fig. 1a are illustrated in Figs. 1b and 1c, respectively.

The results of calculations made for two other injection profiles are shown in Figs. 1d–f and 1g–i. These calculations were made for the "standard bed configuration," an upstream chamber pressure of 100 psia, and an average mass flow rate of 3.0 lb/ft²-sec. The effects on temperature and reactant concentration distributions of a catalyst bed con-

‡ The effects of radial diffusion can be more clearly illustrated with cross plots showing radial temperature profiles at various axial locations in the reactor. Although radial profiles were not plotted for this case, they were plotted for another case discussed later in this section.

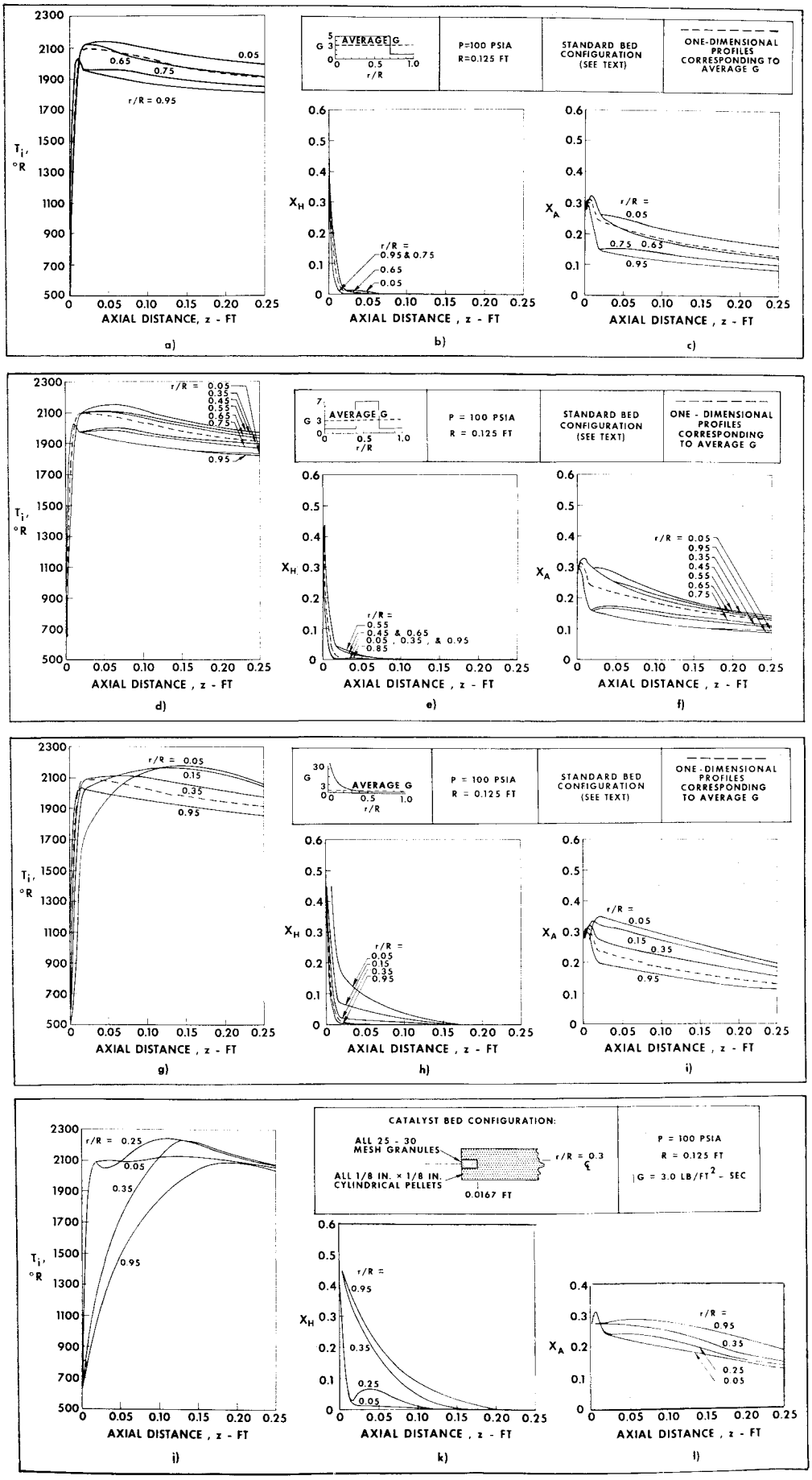

Fig. 1 Steady-state axial profiles of temperature, mole fraction of hydrazine, and mole fraction of ammonia at various radial positions.

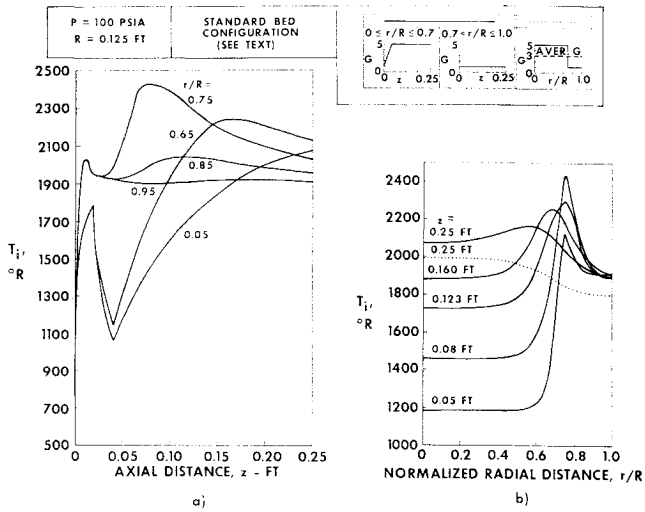

Fig. 2 Steady-state axial and radial temperature profiles for buried injectors.

figuration exhibiting both radial and axial nonuniformities are illustrated in Figs. 1j–l. Here, the mass flow rate was taken as uniform at 3.0 lb/ft²-sec and the upstream chamber pressure was taken as 100 psia.

The effects of the simultaneous turbulent diffusion of heat and mass on temperature and reactant concentration profiles are more clearly indicated for a case in which hydrazine injection is uniform across the inlet face of the reactor but additional hydrazine is introduced into the reactor through

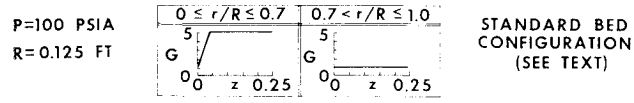

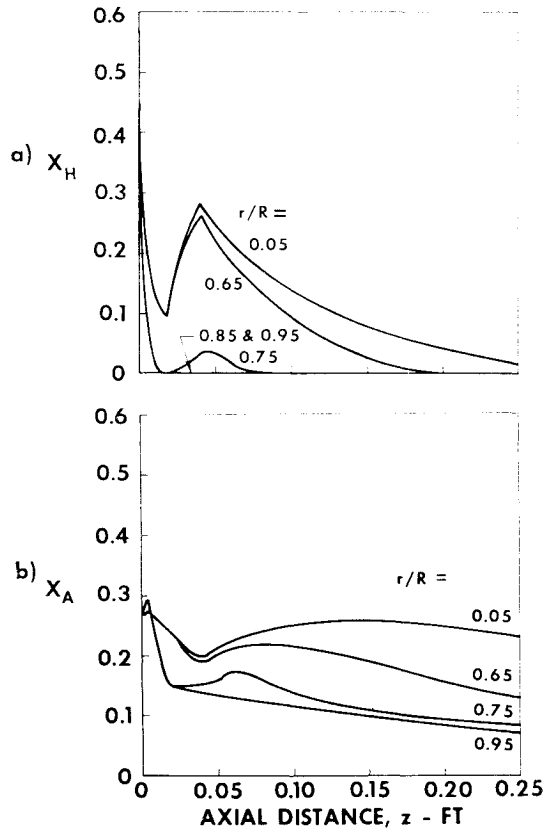

Fig. 3 Steady-state axial profiles of mole-fractions of hydraxine and ammonia at various radial positions for buried injectors.

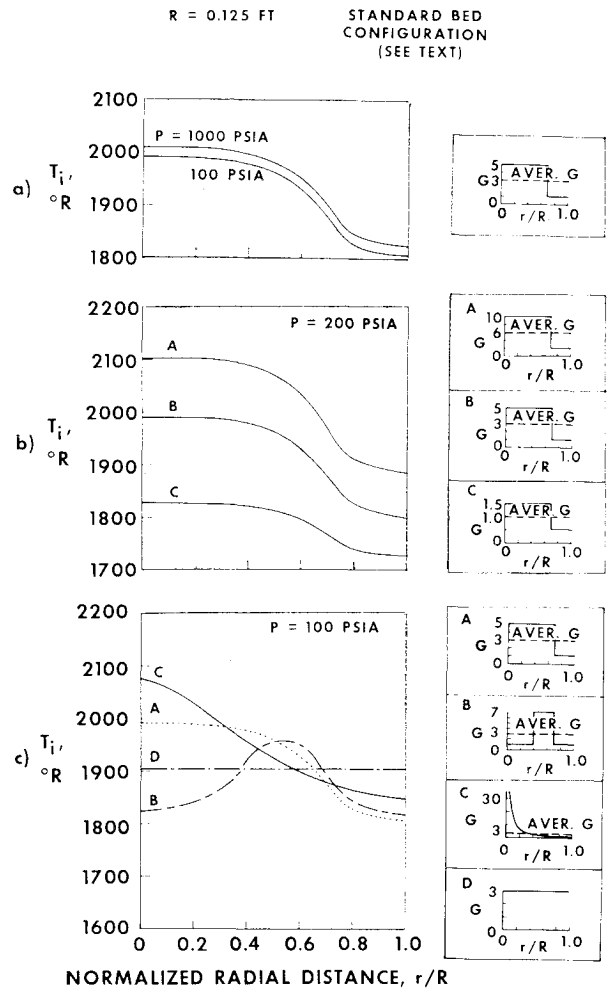

Fig. 4 Effect of pressure, mass flow rate for a given inlet injection profile, and inlet injection profile on steady-state radial temperature profile at exit of 3-in. bed.

injectors imbedded in the catalyst bed. Calculations were made for an injection profile of this type, illustrated in Fig. 2, where the chamber pressure was taken as 100 psia and the bed configurations as "standard." In this case the buried injectors were taken to distribute hydrazine uniformly for $0 \leq r/R \leq 0.7$ over the first $\frac{1}{2}$ in. of the reactor. The calculated temperatures are plotted as a function of axial position at various radial positions in Fig. 2a. Hydrazine diffusion from low- to high-temperature regions results in unusually high temperatures at the interface between the high and low flow rate regions. This results in the formation of a "thermal sheath" which is more clearly illustrated in Fig. 2b, which is a cross plot of the results presented in Fig. 2a. Here temperature is plotted as a function of radial position at various axial locations in the reactor. For comparison purposes, the radial temperature profile at the exit of a 3-in. bed with a step-function (all inlet) injection profile is also plotted in Fig. 2b. The mole-fraction of hydrazine and ammonia distribution associated with these temperature profiles are plotted in Fig. 3.

The effects of various reactor operating conditions on radial temperature profiles at the exit of a 3 in. bed are illustrated in Fig. 4 for the standard bed configuration and for hydrazine injection at the reactor inlet only. The effect of upstream chamber pressure on exit radial temperature profile is shown in Fig. 4a for a step-function injection profile with an average mass flow rate of 3.0 lb/ft²-sec. Very little effect is noted over a ten-fold pressure range. A marked effect of average mass flow rate on radial temperature profile is shown in Fig. 4b for the same step-function injection profile

and an upstream chamber pressure of 200 psia. The effect of inlet injection profile on radial temperature distribution is illustrated in Fig. 4c for an average mass flow rate of 3.0 lb/ft²-sec and an upstream chamber pressure of 100 psia.

It should be noted here that the injection profiles and catalyst bed configurations discussed in this section were chosen simply to illustrate the two-dimensional effects which can occur in the hydrazine reactor. No attempt was made to perform an exhaustive study of the effects of radial variations in reactor operating and design parameters on the steady-state behavior of the reactor system. It is apparent, however, that a one-dimensional model of the system, based on parameters averaged over the reactor cross-section, is not adequate to describe the behavior of a reactor which exhibits significant radial variations in injection profile or bed configuration. For these systems, it is necessary to use the two-dimensional model to effectively predict, for example, the locations of very high-temperature regions such as "thermal sheaths."

References

[1] Kesten, A. S., "Analytical Study of Catalytic Reactors for Hydrazine Decomposition," First Annual Progress Report F910461-12, Contract NAS 7-458, May 1967, United Aircraft Research Labs.

[2] Kesten, A. S., "Analytical Study of Catalytic Reactors for Hydrazine Decomposition—Part I: Steady-State Behavior of Hydrazine Reactors.—Part II: Transient Behavior of Hydrazine Reactors," *Proceeding of the Hydrazine Monopropellant Technology Symposium*, Johns Hopkins Univ., Applied Physics Lab., Silver Spring, Md., Nov. 1967.

[3] Bird, R. B., Stewart, W. E., and Lightfoot, E. N., *Transport Phenomena*, Wiley, New York, 1960.

[4] Argo, W. B. and Smith, J. M., "Heat Transfer in Packed Beds," *Chemical Engineering Progress*, Vol. 49, 1953, pp. 443–451.

[5] Prater, D. C., "The Temperature Produced by Heat of Reaction in the Interior of Porous Particles," *Chemical Engineering Science*, Vol. 8, 1958, pp. 284–286.

[6] Kesten, A. S., "An Integral Equation Method for Evaluating the Effects of Film and Pore Diffusion of Heat and Mass on Reaction Rates in Porous Catalyst Particles," *AIChE Journal*, Vol. 15, 1969, pp. 128–131.

[7] Smith, E. J., Smith, D. B., and Kesten, A. S., "Analytical Study of Catalytic Reactors for Hydrazine Decomposition—Computer Programs Manual—One- and Two-Dimensional Steady-State Programs," Rept. G910461-30, Contract NAS 7-458, Aug. 1968, United Aircraft Research Labs.